ACS APPLIED MATERIALS & INTERFACES

Research Article

www.acsami.org

Conformal Electroplating of Azobenzene-Based Solar Thermal Fuels onto Large-Area and Fiber Geometries

David Zhitomirsky and Jeffrey C. Grossman*

Department of Materials Science and Engineering, Massachusetts Institute of Technology, Cambridge, Massachusetts 02139, United States

Supporting Information

ABSTRACT: There is tremendous growth in fields where small functional molecules and colloidal nanomaterials are integrated into thin films for solid-state device applications. Many of these materials are synthesized in solution and there often exists a significant barrier to transition them into the solid state in an efficient manner. Here, we develop a methodology employing an electrodepositable copolymer consisting of small functional molecules for applications in solar energy harvesting and storage. We employ azobenzene solar thermal fuel polymers and functionalize them to enable deposition from low concentration solutions in methanol, resulting in uniform and large-area thin films. This approach enables conformal deposition on a variety of conducting substrates that can be either flat or structured depending on the application. Our approach further enables control over film growth via electrodepsition conditions and results in highly uniform films of hundreds of nanometers to microns in thickness. We demonstrate that this method enables superior retention of solar thermal fuel properties, with energy densities of ∼90 J/g, chargeability in the solid state, and exceptional materials utilization compared to other solid-state processing approaches. This novel approach is applicable to systems such as photon upconversion, photovoltaics, photosensing, light emission, and beyond, where small functional molecules enable solid-state applications.

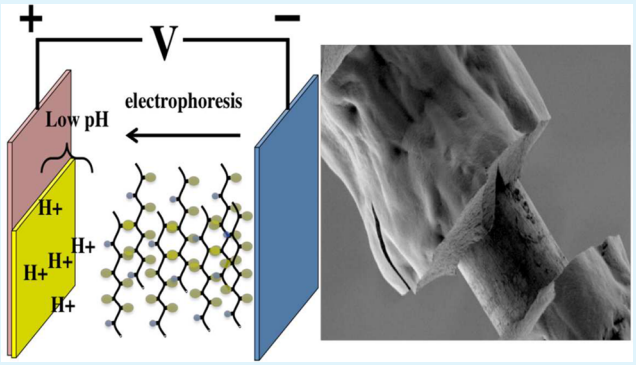

KEYWORDS: *electrodeposition, solar thermal fuels, polymers, thin-films, azobenzene*

INTRODUCTION

Solar energy is one of the most energetic and abundant renewable resources available on Earth. Collecting this energy typically involves an active material that can transduce photons into other useful types of energy, where a specific form factor is required to maximize the efficiency of energy harvesting and utilization. For example, colloidal quantum dots are synthesized in solution and are excellent solar absorbers, but require to be deposited into solid-state arrays to transport the resultant charges.[1,2] Alternatively, organic dyes can simply be deposited as a monolayer on a semiconducting metal oxide while also being immersed in an electrolyte to facilitate charge collection, as is done in dye-sensitized solar cells.[3,4] Molten salts must undergo a phase transition in order to store solar heat energy efficiently,[5] and recently reported novel solar thermal fuel (STF) materials may be employed in both solution and solid-state to accomplish simultaneous energy conversion and storage.[6−8]

An STF molecule such as azobenzene can undergo *trans* to *cis* isomerization upon absorption of an appropriate UV energy photon, whereby energy is stored within the conformation of the molecule, and can later be retrieved as heat. We recently reported that integrating STFs within the solid-state form factor opens an avenue toward implementation in solid-state energy devices for heat release applications.[6] This was accomplished through a facile solution spin-coating deposition process of polymer materials that resulted in uniform thin-films. However, this deposition method results in geometry constraints that limit chargeability, thickness, heat release, and heat propagation within the resultant solid-state devices. Furthermore, spin-coating requires a high solubility of the material in the chosen solvent and is prone to result in a large fraction (>90%) of the active material being wasted. Increasing the versatility of these materials will require flexibility of their deposition on arbitrary form factors with controllable thickness and high materials utilization.

Electrodeposition (EPD) onto conducting materials enables utilization of a variety of form factors, is conformal, can employ solutions at low concentrations, and maximizes utilization yield. This facile process requires the material of interest to be dissolved in an electrolyte and bias to be applied between working and counter electrodes to force the dissolved species to migrate and deposit on oppositely charged electrodes. By controlling the deposition conditions (applied voltage or

Received: July 1, 2016
Accepted: September 9, 2016
Published: September 9, 2016

DOI: 10.1021/acsami.6b08034
ACS Appl. Mater. Interfaces 2016, 8, 26319−26325

current), it is possible to tune thickness and film morphology. Furthermore, the method is highly scalable, relatively inexpensive, and does not require a complex infrastructure. EPD has recently been used in a variety of energy related applications spanning electrodes for batteries[9−11] and supercapacitors,[12,13] and active layer deposition in solar cells.[14,15] Here we report a novel STF polymer material that can be readily deposited via EPD onto a variety of substrates in a conformal fashion by copolymerizing an azobenzene monomer with a carboxylic acid-based monomer to enable charging (and thus response to an electric field) of the resultant copolymer in solution. We furthermore present novel device concepts involving fiber geometries that offer the potential to efficiently store solar energy and transport heat within STF fibers.

EXPERIMENTAL SECTION

STF Monomer Synthesis. The monomer was synthesized based on a published recipe.[16] Briefly, p-(phenylazo)phenol ($C_{12}H_{10}N_2O$, 2g, 0.01 mol) was dissolved in tetrahydrofuran (THF, 25 mL) and triethylamine ($C_6H_{15}N$, 1.4 mL, 0.01 mol) in anhydrous and oxygen free conditions. Methacryloyl chloride (C_4H_5ClO, 3 mL, 0.031 mol) was added dropwise under inert conditions, while cooling reaction in an ice bath (resulting in gas evolution, dark color change, and salt precipitate). The reaction was left stirring at room temperature for 48 h. Extraction was done by diluting four times with 3:1 mix of dichloromethane (DCM) (or chloroform) and water. The organic phase was dried with sodium sulfate (Na_2SO_4) and dried under vacuum (<0.1 mbar) overnight. The resultant material was purified in a silica column using 1:1 DCM:hexanes. Overall reaction yield is between 70 and 80%.

Polymer Synthesis. In a typical copolymerization, the STF monomer and charging unit (4-vinylbenzoic acid, $C_9H_8O_2$) were combined at a 5:1 molar ratio, based on 100 mg (0.38 mmol) of monomer. This combination was dissolved in anhydrous THF (1 mL) and 2,2′-Azobis(2-methylpropionitrile) ($C_8H_{12}N_4$, 3 mg, 0.02 mmol) was added. The solution was subjected to 3 freeze/pump/thaw cycles. The reaction was run under inert conditions at 65 °C for 3 h. The polymer was isolated in a solution of stirred methanol, and then filtered and rinsed with additional methanol. The reaction is easily scaled to 1 g. Maximum yields obtained were 50%.

Electrodeposition. Twenty milligrams of polymer were combined with 40 mL of methanol to give a concentration of 0.5 mg mL^{-1}. A concentrated (pH ∼14) solution of KOH in methanol was used to adjust the pH of the polymer solution to between 8 and 9. A small amount of deionized water (100 μL) was added to enable continuous films. Stainless steel electrodes were cut from Corrosion Resistant 316 Stainless Steel foil 004″ in thickness. The electrodes were placed opposite each other at a separation of 2 cm, with an immerse area of ∼3.2 cm^2. A constant voltage power supply was used to apply voltages up to 10 V. The best planar films were obtained at 5 V with deposition time of 3 min, with current densities approximately 0.1−0.3 mA cm^{-2}. Corrsion Resistant 304 Stainless Steel Woven Wire Cloth 400 × 400 Mesh, 0.001′ Wire, 40 × 40 Mesh, 0.01″ Wire and 15 × 15 Mesh, 0.01″ Wire were used for depositing on three-dimensional geometries with similar deposition parameters. 0.002″ wire was used for constructing the STFibs, though deposition times need to be reduced to 1−2 min to prevent overly thick deposits.

UV−Vis Measurements of Solid-State Films. Absorption was carried out using a Cary 5000 on films deposited on ITO substrates. Sample charging was done using a high power UV lamp at a distance of 10 cm (100 W). Discharging of films was carried out via heating at 130 °C. For time dependent charging measurements, the film was charged as described above and then transported in the dark for absorption spectrum measurement. For time-dependent discharging measurements, the film was left in the spectrophotometer in the dark and measured at fixed time intervals over 18 h.

Image Acquisition. Film photographs were obtained using a conventional optical microscope. High magnification images and cross sections were obtained using a Zeiss Merlin scanning electron microscope with the settings show in the manuscript figures (typically 1−2 keV and ∼100 pA, working distance of 3−4 mm).

Charging and Differential Scanning Calorimetry. Solution samples in acetone were charged using a 365 nm 100 W UV lamp while cooled at 25 °C while stirring. Solid-state samples were kept at 30 °C using a cooling stage while charged using the 100 W lamp at a distance of 10 cm. Films were subsequently redissolved in acetone for sample preparation for calorimetry. The solutions were dried in differential scanning calorimetry (DSC) pans in the dark and sealed, giving a final mass of ∼1 mg of material. DSC was carried out using a TA Instruments DSC Q20 at a scan rate of 10 °C/min.

Size Exclusion Chromatography. SEC measurements were performed on 0.5 mg mL − 1 samples in stabilized, High Performance Liquid Chromatography (HPLC)-grade THF using an Agilent 1260 Infinity system with variable-wavelength diode array (254, 450, and 530 nm) and refractive index detectors, guard column (Agilent PLgel; 5 μm; 50 mm × 7.5 mm), and three analytical columns (Agilent PLgel; 5 μm; 300 mm × 7.5 mm; 105, 104, and 103 Å pore sizes). The instrument was calibrated with narrow-dispersity polystyrene standards between 1.7 and 3150 kg mol^{-1}. All runs were performed at 1.0 mL min −1fl ow rate and 35 °C. Molecular weight values were calculated using Chemstation Gel Permeation Chromatography Data Analysis Software (Rev. B.01.01) based on the refractive index signal.

RESULTS

STF are most commonly deployed as small-molecule photoswitches, sometimes anchored to additional structures for enhanced properties.[6,17−19] We chose to create an azobenzene-based STF for EPD due to its recent success with respect to its charging, cycling and energy density properties.[6] Literature reports remain sparse with respect to EPD of small molecules and azobenzene-containing moieties in particular.[20,21] Generally, in order to deposit robust EPD films, a high molecular weight polymer is desirable. In one approach an EPD procedure was developed for commercially available azobenzene-containing Poly[1-[4-(3-carboxy-4-hydroxyphenylazo)-benzenesulfonamido]-1,2-ethanediyl] by employing the inherent negatively charged ionic group that could respond to applied electric field.[22] However, we found that this polymer did not exhibit favorable solar thermal fuel properties in terms of energy density or chargeability. In fact, it was found that the additional functional groups decorating the benzene rings of the azobenzene molecule that impart the favorable EPD properties, simultaneously limit its energy storage by greatly curtailing the storage lifetime.[23,24] In effect, any modification of the azobenzene molecule to impart new properties (such as those required for EPD) can often negatively affect its STF characteristics.

We took the view that engineering a novel polymer material would enable success in the EPD of STF coatings, but would also require a robust strategy of incorporating ionizable moieties without perturbing the azobenzene chemical structure. Engineering such a polymer would ideally preserve all the beneficial energy harvesting and storage properties developed for previously reported solid-state azobenzene films.[6] Additionally, it would be beneficial to retain the facile two-step synthesis process, yield and scalability. To achieve this, we have developed a copolymer consisting predominantly of an azobenzene monomer and a sparsely incorporated 4-vinylbenzoic acid charging unit (Figure 1a). Because the charging unit does not contribute to the stored energy density, its content in the polymer should be minimized while still enabling efficient EPD. At neutral pH and acidic pH, such a polymer will ideally be insoluble in the electrolyte, whereas at a high pH, it

DOI: 10.1021/acsami.6b08034
ACS Appl. Mater. Interfaces 2016, 8, 26319−26325

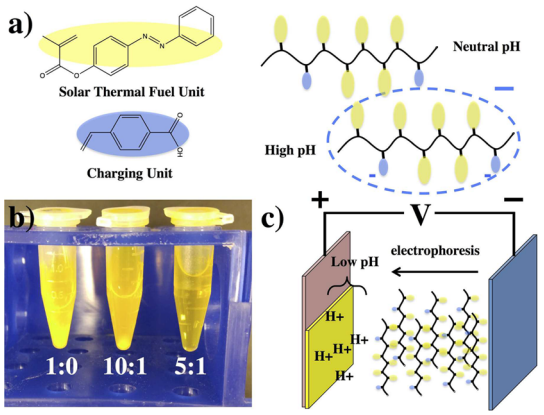

Figure 1. Solar thermal fuel copolymer for electrodeposition. (a) Structures representing the solar thermal fuel and charging units. Incorporation of these units into a copolymer enables to change the charge and thus solubility based on the pH, thus enabling to generate solid-state coatings under neutral or low pH conditions. (b) Photograph depicting the solubility of various synthesized polymers based on solar thermal fuel: charging unit ratio. At low charging unit concentrations, even at high pH, the polymer cannot dissolve evident by the turbid solution, whereas at 5:1, the solution becomes clear indicating solubility. (c) Concept of the electrodeposition scheme, where the charged polymer in basic solution migrates in response to an electric field and deposits on the positive electrode where protons are generated, thus enabling a pH drop.

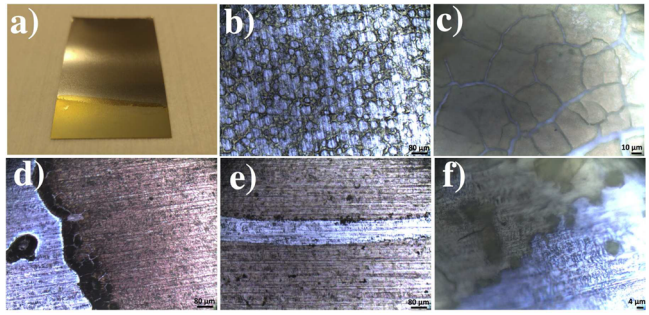

Figure 2. Optical microscopy of solid-state films. (a) Optimized solar thermal fuel solid-state film deposited on stainless steel represented by the yellow coated portion. (b) Discontinuous film formed as a result of lack of protons, necessecitating the addition of a small amount of water to the solution. (c) Effect of longer deposition times (>10 min at 5 V), where film forms cracks upon drying. (d) Optical microscope image of boundary of film between the stainless steel and film region, where careful optimization results in a continuous coating (see methods). (e) The film in d scratched near the center to ascertain smoothness based on contrast with the underlying electrode. (f) Higher-magnification image of the scratch at the interface, depicting a well-connected and continuous film.

should readily dissolve and migrate in response to an electric field.[25] We screened several compositions of such a polymer, and in Figure 1b show the methanol solubility with increasing charging unit percentage. At a ratio of 5:1 (azobenzene to charging unit), the polymer can be readily dissolved upon adjusting the pH to ~8−9, while at neutral or acidic pH values it remains insoluble. A simple radical polymerization reaction with a yield of ~50% can reproducibly generate this material. We find that the molecular weight of our polymer is approximately 4.3×10^3 g/mol (Figure S1), which is within the same order or magnitude as previously reported azobenzene homopolymers.[6] Once dissolved, the polymer can be electroplated onto the positive electrode from methanol with application bias in the rage of 5 to 10 V on a variety of conductive electrodes. The process proceeds by the ionized carboxyl groups causing the polymer to migrate to the anode, where a surplus of cations causes a pH change and the polymer becomes insoluble thus forming a solid-state coating (Figure 1c).

Solid-state coatings were fabricated using the EPD process on stainless steel electrodes with the application of bias at time scales of 1−10 min. Optimized films on the order of 500−1000 nm in thickness (methods) were achieved and a sample film is shown in Figure 2a. The film makes a uniform reflective, semitransparent yellow coating on the submerged (active) area of the electrode. However, this cannot be readily achieved from utilizing the as-prepared methanol-polymer solution, as instead of uniform films, the resultant coating exhibits patchy and disconnected regions (Figure 2b). A small (~0.25% by vol) amount of H_2O is required to enable water-splitting at the anode that generates protons and forces the pH drop. Similarly, poor film morphology results if extended periods of time are used for deposition, as the film begins to form cracks and disconnected regions upon drying, though the individual regions exhibited uniformity (Figure 2c). Microscope images show the interface regions between coated and uncoated portions of the film at the edge of the submerged portion (Figure 2d) and at the interface where an intentional scratch has been made in the film (Figure 2e). Evidently, at these low optical magnifications, the film is uniform and continuous. Higher magnification at the scratch interface further exhibits the film existing as a uniform and connected layer (Figure 2f).

EPD offers the unique advantage of conformal deposition as the electric field is applied through the active electrode area. In this respect EPD has often been a popular choice for nanostructing where high aspect ratios are needed, such as in nanowire solar cell designs.[26,27] To further probe our EPD polymer approach, we deposited our material on a series of stainless steel meshes of varying wire thickness (Figure 3). Figure 3a shows that the EPD approach can coat the active area effectively as evident from the color contrast with the uncoated portions. To ascertain whether the coating was conformal, we carried out scanning electron microscopy. At a low deposition time (3 min) and using the finest mesh (25 μm wire), the deposition was conformal and coated the mesh evenly as evident from Figure 3b. Extending the deposition time further resulted in delamination of the coatings, however the conformity to the shape of the mesh was retained (Figure 3c). Evidently, this materials platform enables deposition on three-dimensional geometries that may become quite useful for nanoscopic and microscopic devices that utilize STF as well as larger macroscopic solid-state devices.

DISCUSSION

The polymer EPD approach shows promise for integrating STFs into solid-state devices where large area and tunable thickness are achievable by simple manipulation of the deposition parameter space. Furthermore, a variety of geometries can be utilized depending on the application, which enables us to envision some microscopic devices such as heat-triggered degradable electronics and drug delivery.[28,29] On the macroscale, it enables combining STFs with fine metallic structures, such as wires, to enables solar thermal fibers (STFibs) that could leverage the high thermal conductance of

DOI: 10.1021/acsami.6b08034
ACS Appl. Mater. Interfaces 2016, 8, 26319−26325

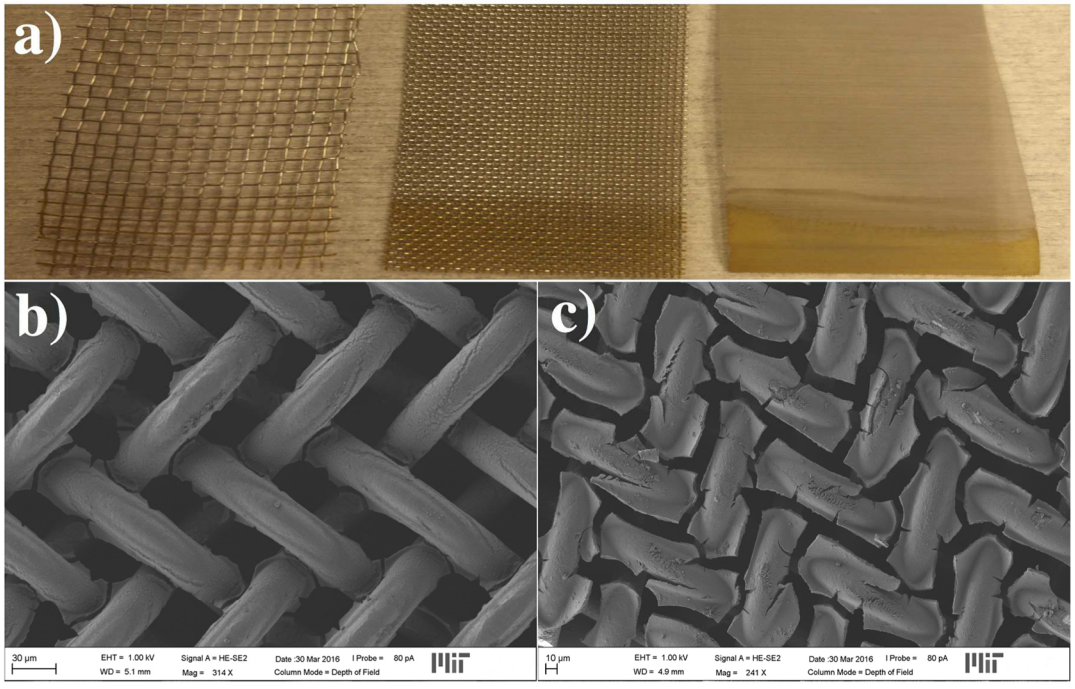

Figure 3. Deposition on three-dimensional structures. (a) Wire meshes (250 to 25 μm wire thickness) with STF deposits on the lower edge represented by the yellow hue. (b) Scanning electron microscopy image of the 25 μm mesh with a thin STF coating conformably coating the wires (3 min of deposition, see methods). (c) Image of the 25 μm mesh with a thicker coating achieved by extending the deposition time (8 min). Crack formation and delamination occurs for thicker coatings, similar to Figure 2c.

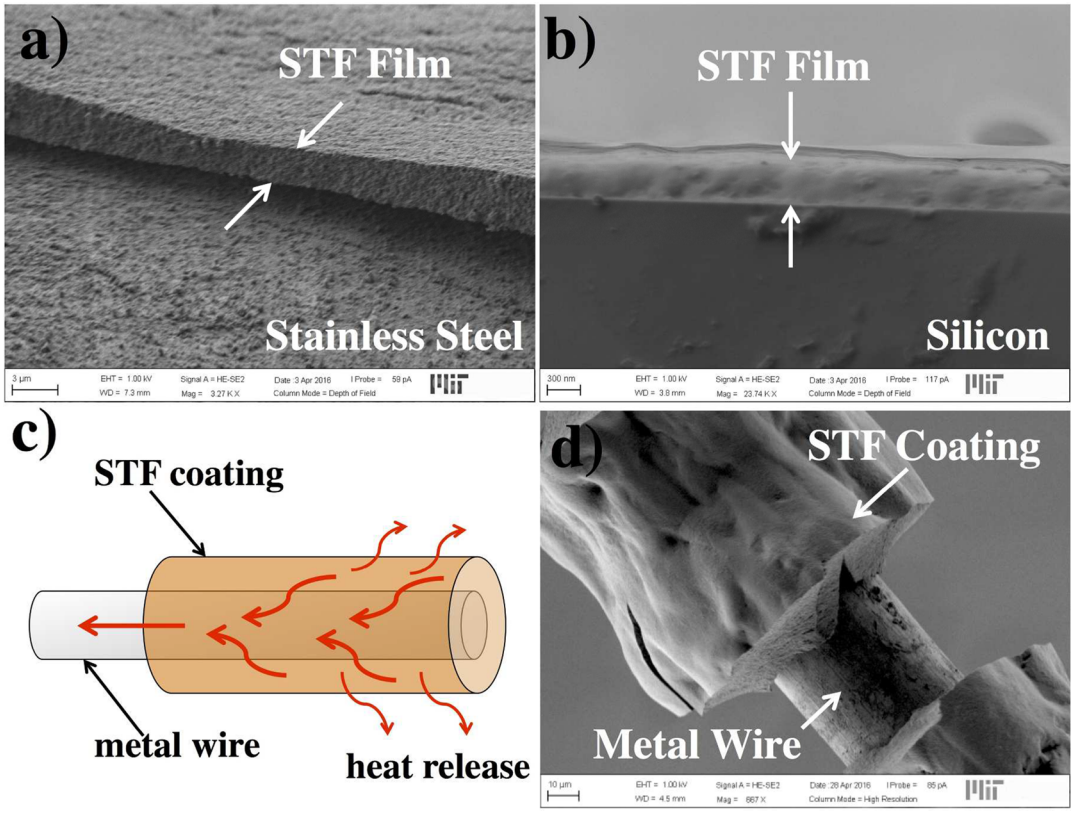

Figure 4. Film uniformity and applications. (a) Scanning electron microscopy cross-section image of an electrodeposited film on stainless steel. (b) Scanning electron microscopy cross-section image of an electrodeposited film on a silicon substrate. (c) Concept for a solar thermal fuel fiber where solar energy is stored within the fiber and released as heat into the wire to be carried off elsewhere within a functional device. (d) Proof-of-concept using an electrodeposited thick solar thermal fuel coating atop a 50 μm fiber depicting both the wire and the copolymer coating.

DOI: 10.1021/acsami.6b08034
ACS Appl. Mater. Interfaces 2016, 8, 26319−26325

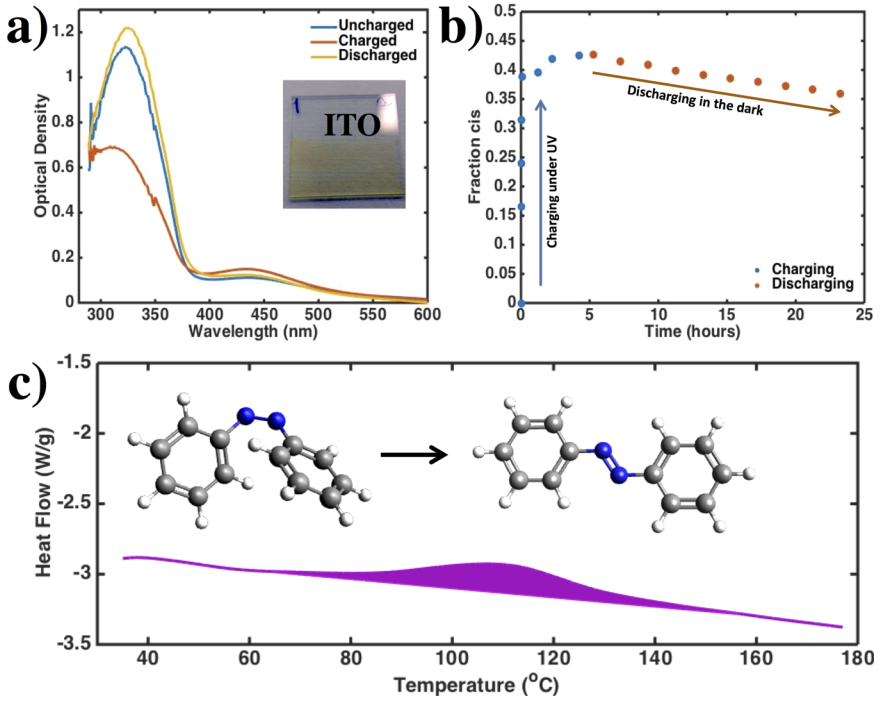

Figure 5. Optical and thermal response of the solar thermal fuel copolymer. (a) Absorbance spectrum of the copolymer electrodeposited solar thermal fuel film atop of conductive indium tin oxide/glass substrate. Response after charging shown in red, where the peak magnitude decreases because of an increase in the *cis* fraction and a decrease in the *trans*. Discharging the film results in the recovery of the initial peak due to restoration of the *trans* population. (b) Charging and discharging as a function of time monitored by absorption spectroscopy. (c) Scanning differential calorimetry carried out on the charged copolymer, whereby the *cis* isomer is converted to the *trans* variant (depicted). A heat release corresponding to a gravimetric energy density of 90 J g^{-1} is observed.

metals for heat delivery and management. This greatly expands the opportunity space for integrating STFs into functional devices. More broadly, this type of copolymer EPD approach for small molecules represents a systematic way of controlled and conformal electroplating of functional materials onto a variety of substrates and form factors.

To show the applicability of the materials across various substrates and length scales for device applications, we investigated cross-sectional samples to ascertain film smoothness and uniformity. Figure 4a shows a cross-section region on a stainless-steel electrode, where a film uniform in thickness is shown, as well as having uniform morphology. The film is on the order of a few micrometers, and forms an independent layer as seen slightly lifting off the substrate. It is worth noting that the surface of the stainless steel has a roughness of several hundred nanometers to a micron, thus the morphology may be improved with a smooth substrate. We next turn to N-doped crystalline silicon as the electrode, exhibiting exceptionally low roughness (<1 nm), where an SEM image (Figure 4b) depicts a much more uniform film with a thickness of ∼350 nm. We found longer deposition times and higher voltages were necessary compared to stainless steel in order to deposit a thick layer atop of silicon, likely due to the lower electrode conductivity of the latter.

On the basis of our analysis of the polymer EPD and the resultant coatings, it is possible to propose a potential application in the form of a STFib, where a thin (∼50 μm) metal wire is coated with the STF material and integrated into fabrics. Seeing as the STF polymer itself has a low thermal conductivity (<1 W mK^{-1}), combination with high thermal conductivity metals (up to 400 W mk^{-1} for copper) could allow for efficient transport of heat to other parts of the fabric or device, as the active area exposed to photon radiation and the region that requires heat may not necessarily be overlapping. The STF would charge with UV radiation, and then when triggered would release heat into the wire that would enable other portions of the device or fabric to be heated (Figure 4c). In Figure 4d, we depict such a wire (∼50 μm) where an STF coating has been deposited as a proof-of-concept for such an STFib. The deposition conditions were optimized to achieve thick coatings (on the same order of the wire thickness), but similar to Figure 2c, at higher thicknesses there is greater film shrinkage during drying and cracks and deformities may be introduced. We expect engineering higher molecular weight polymers or adding binders may serve as a remedy, which is a promising future direction for the optimization of such fiber materials. Finally, we discuss the implications of employing copolymers and their impact on STF performance. We previously reported a homopolymer comprised of azobenzene units with an energy density of ∼100 J g^{-1}.[6] To impart novel functionality, in this work, we incorporate the charging units that in turn add nonproductive mass to the system from an energy storage point of view. For our polymer with 5:1 ratio, this represents an 8% reduction in the potential energy density. In effect, to avoid the much greater compromises associated with modifying the azobenzene molecule itself, we instead opt for a small compromise that offers a robust and scalable platform to impart new properties to our materials. To ascertain whether the STF properties are preserved, we perform optical and thermal studies on the STF copolymer (Figure 5). The EPD process results in a semitransparent yellow film on indium-doped tin oxide (Figure 5a inset), and it readily photoswitches and reverts to its original state in the

DOI: 10.1021/acsami.6b08034
ACS Appl. Mater. Interfaces 2016, 8, 26319−26325

solid state as evident by the change in magnitude of the $\pi \rightarrow \pi^*$ (~325 nm) transition in the absorption spectrum.

We investigate the time-dependent charging properties of a film of optical density of 1.4 at the $\pi-\pi^*$ transition (thickness ~250 nm). An uncharged *trans*-dominant film is exposed to a 365 nm radiation source and the optical density monitored as a functional of time. From these data we extract the fraction of *cis* isomer (Figure S2) and plot it as a function of time (Figure 5b). The film charges rapidly approaching saturation in just 30 min, and after approximately 4 h a photostationary state is reached where the spectrum no longer changes on practical time scales of 1−2 h (<2% absorption change). At the defined photostationary state, 43% of the film has been converted to the *cis* isomer. We then monitor the charged film in the dark at room temperature as it thermally reverts back to the *trans* state. The fraction of *cis* isomer is plotted as a function of time in Figure 5b alongside the photocharging data. By analyzing the spectral decay rate (Figure S3) it is found that the *cis* state within the film has a half-life of 75 h which would be suitable for a host of short-term applications, such as integration into wearable fabrics. Differential Scanning Calorimetry measurements (Figure 5c) reveal that the energy density is well retained (~90 ± 5 J g^{-1}), which is consistent based on the quantity of charging unit employed per unit of azobenzene. Evidently, this first report of an energy storing STF copolymer film achieved via electrodeposition serves to exemplify incorporation of new functionality into STF materials with minimal compromises.

Finally, we discuss the glass transition temperature (T_g) as it relates to operation of STF thin-films. Literature reports have attempted to blend azobenzene into poly(methyl methacrylate) as pristine azobenzene crystallizes and does not result in photoswitchable films.[30] In these experiments it is found that blends with lower T_g result in more rapid charging due to increased conformational freedom for azobenezene. Our polymer approach similarly enables formation of amorphous films with potentially low T_g values due to low chain stiffness and low polymer molecular weight (Figure S1). We measure T_g in our materials using DSC (Figure S4) to be approximately 7 °C. For applications requiring lower temperatures, charging may be hindered if done below T_g, thus strategies such as adding flexible pendant groups to disrupt chain packing and choosing comonomers not susceptible to intermolecular forces would aid in lowering T_g.

Our approach enables electrodeposition of STF materials, but it may be applied to a broader suite of functional molecules. In other fields, such as photon upconversion, there has been a recent push to extend the capabilities of solid-state photon upconverting thin-films for device applications.[31,32] So much so, that a similar approach was taken in introducing pendant emitter and sensitizer moieties onto a polymer backbone,[33] where now the potential addition of a charging unit could similarly predispose the polymer for EPD, enabling the same processing benefits.

CONCLUSIONS

EPD offers an exciting avenue for deposition of STFs onto a variety of substrates and form factors to give rise for novel applications. Additionally, EPD allows for controllable deposition over large areas and with tunable thickness, and greatly enhances the materials utilization efficiency; however, modification of the STF molecules themselves often comes at a large compromise to their energy storage properties. The copolymer STF approach is a robust and precise way of enhancing the STF functionality for novel solid-state applications without major compromises to the energy density. Additional functional groups and molecules may easily be incorporated into the material, while minimally affecting the STF energy storage functionality. Beyond charging units for EPD, moieties may be included to enable cross-linking to form freestanding films, broader solar absorption, and enhanced energy density through side-chain interactions.[34] We show that together with the EPD approach, the copolymer can conformally deposit onto three-dimensional architectures, enables smooth and uniform film morphology, and enables new applications such as STFibs that may be employed in fabrics or other solid-state devices with specific requirements on heat storage and transport. Beyond STFs, the copolymer EPD approach potentially enables fabrication of solid-state films with any functional small-molecule and represents a broad spectrum of opportunities for novel solid-state devices. It is expected that this work would be widely applicable to research where small molecules, polymers, and solid-state films are necessary, and tremendously enhances the versatility with which STFs in particular may be deployed for industrial and consumer applications.

ASSOCIATED CONTENT

Supporting Information

The Supporting Information is available free of charge on the ACS Publications website at DOI: 10.1021/acsami.6b08034.

Photocharging of solid-state films, photostationary state analysis, thermal back-reversion, differential scanning calorimetry at low temperature, and size exclusion chromatography of the polymer samples (PDF)

AUTHOR INFORMATION

Corresponding Author

*E-mail: jcg@mit.edu.

Notes

The authors declare no competing financial interest.

ACKNOWLEDGMENTS

D.Z. acknowledges his Natural Sciences and Engineering Research Council of Canada Banting Fellowship. Materials and resources funding for this project was provided by Bavarian Motor Works (BMW).

REFERENCES

(1) Choi, J.-H.; Wang, H.; Oh, S. J.; Paik, T.; Sung, P.; Sung, J.; Ye, X.; Zhao, T.; Diroll, B. T.; Murray, C. B.; Kagan, C. R. Exploiting the Colloidal Nanocrystal Library to Construct Electronic Devices. *Science* **2016**, *352* (6282), 205−208.

(2) Kim, J. Y.; Voznyy, O.; Zhitomirsky, D.; Sargent, E. H. 25th Anniversary Article: Colloidal Quantum Dot Materials and Devices: A Quarter-Century of Advances. *Adv. Mater.* **2013**, *25* (36), 4986−5010.

(3) Hardin, B. E.; Snaith, H. J.; McGehee, M. D. The Renaissance of Dye-Sensitized Solar Cells. *Nat. Photonics* **2012**, *6* (3), 162−169.

(4) Docampo, P.; Guldin, S.; Leijtens, T.; Noel, N. K.; Steiner, U.; Snaith, H. J. Lessons Learned: From Dye-Sensitized Solar Cells to All-Solid-State Hybrid Devices. *Adv. Mater.* **2014**, *26* (24), 4013−4030.

(5) Bauer, T.; Pfleger, N.; Breidenbach, N.; Eck, M.; Laing, D.; Kaesche, S. Material Aspects of Solar Salt for Sensible Heat Storage. *Appl. Energy* **2013**, *111*, 1114−1119.

(6) Zhitomirsky, D.; Cho, E.; Grossman, J. C. Solid-State Solar Thermal Fuels for Heat Release Applications. *Adv. Energy Mater.* **2016**, *6* (6), 1502006.

DOI: 10.1021/acsami.6b08034
ACS Appl. Mater. Interfaces 2016, 8, 26319−26325

(7) Kucharski, T. J.; Ferralis, N.; Kolpak, A. M.; Zheng, J. O.; Nocera, D. G.; Grossman, J. C. Templated Assembly of Photoswitches Significantly Increases the Energy-Storage Capacity of Solar Thermal Fuels. *Nat. Chem.* **2014**, *6* (5), 441−447.
(8) Börjesson, K.; Ćoso, D.; Gray, V.; Grossman, J. C.; Guan, J.; Harris, C. B.; Hertkorn, N.; Hou, Z.; Kanai, Y.; Lee, D.; Lomont, J. P.; Majumdar, A.; Meier, S. K.; Moth-Poulsen, K.; Myrabo, R. L.; Nguyen, S. C.; Segalman, R. A.; Srinivasan, V.; Tolman, W. B.; Vinokurov, N.; Vollhardt, K. P. C.; Weidman, T. W. Exploring the Potential of Fulvalene Dimetals as Platforms for Molecular Solar Thermal Energy Storage: Computations, Syntheses, Structures, Kinetics, and Catalysis. *Chem. - Eur. J.* **2014**, *20* (47), 15587−15604.
(9) Ortiz, G. F.; López, M. C.; Alcántara, R.; Tirado, J. L. Electrodeposition of Copper−tin Nanowires on Ti Foils for Rechargeable Lithium Micro-Batteries with High Energy Density. *J. Alloys Compd.* **2014**, *585*, 331−336.
(10) Ponrouch, A.; Frontera, C.; Barde, F.; Palacin, M. R. Towards a Calcium-Based Rechargeable Battery. *Nat. Mater.* **2016**, *15* (2), 169−172.
(11) Zhao, Q.; Hu, X.; Zhang, K.; Zhang, N.; Hu, Y.; Chen, J. Sulfur Nanodots Electrodeposited on Ni Foam as High-Performance Cathode for Li−S Batteries. *Nano Lett.* **2015**, *15* (1), 721−726.
(12) Li, X.; Zhitomirsky, I. Electrodeposition of Polypyrrole−carbon Nanotube Composites for Electrochemical Supercapacitors. *J. Power Sources* **2013**, *221*, 49−56.
(13) Chen, W.; Xia, C.; Alshareef, H. N. One-Step Electrodeposited Nickel Cobalt Sulfide Nanosheet Arrays for High-Performance Asymmetric Supercapacitors. *ACS Nano* **2014**, *8* (9), 9531−9541.
(14) Ahmed, S.; Reuter, K. B.; Gunawan, O.; Guo, L.; Romankiw, L. T.; Deligianni, H. A High Efficiency Electrodeposited Cu2ZnSnS4 Solar Cell. *Adv. Energy Mater.* **2012**, *2* (2), 253−259.
(15) Jeon, J.-O.; Lee, K. D.; Seul Oh, L.; Seo, S.-W.; Lee, D.-K.; Kim, H.; Jeong, J.; Ko, M. J.; Kim, B.; Son, H. J.; Kim, J. Y. Highly Efficient Copper−Zinc−Tin−Selenide (CZTSe) Solar Cells by Electrodeposition. *ChemSusChem* **2014**, *7* (4), 1073−1077.
(16) Moniruzzaman, M.; Sabey, C. J.; Fernando, G. F. Synthesis of Azobenzene-Based Polymers and the in-Situ Characterization of Their Photoviscosity Effects. *Macromolecules* **2004**, *37* (7), 2572−2577.
(17) Lennartson, A.; Roffey, A.; Moth-Poulsen, K. Designing Photoswitches for Molecular Solar Thermal Energy Storage. *Tetrahedron Lett.* **2015**, *56* (12), 1457−1465.
(18) Kucharski, T. J.; Tian, Y.; Akbulatov, S.; Boulatov, R. Chemical Solutions for the Closed-Cycle Storage of Solar Energy. *Energy Environ. Sci.* **2011**, *4* (11), 4449−4472.
(19) Luo, W.; Feng, Y.; Cao, C.; Li, M.; Liu, E.; Li, S.; Qin, C.; Hu, W.; Feng, W. A High Energy Density Azobenzene/graphene Hybrid: A Nano-Templated Platform for Solar Thermal Storage. *J. Mater. Chem. A* **2015**, *3* (22), 11787−11795.
(20) Allwright, E.; Berg, D. M.; Djemour, R.; Steichen, M.; Dale, P. J.; Robertson, N. Electrochemical Deposition as a Unique Solution Processing Method for Insoluble Organic Optoelectronic Materials. *J. Mater. Chem. C* **2014**, *2* (35), 7232−7238.
(21) Zhao, R.; Zhan, X.; Yao, L.; Chen, Q.; Xie, Z.; Ma, Y. Electrochemical Deposition of Azobenzene-Containing Network Films with High-Contrast and Stable Photoresponse. *Macromol. Rapid Commun.* **2016**, *37* (7), 610−615.
(22) Liu, Y.; Luo, D.; Zhang, T.; Shi, K.; Wojtal, P.; Wallar, C. J.; Ma, Q.; Daigle, E. G.; Kitai, A.; Xu, C.-Q.; Zhitomirsky, I. Film Deposition Mechanisms and Properties of Optically Active Chelating Polymer and Composites. *Colloids Surf., A* **2015**, *487*, 17−25.
(23) Dokić, J.; Gothe, M.; Wirth, J.; Peters, M. V.; Schwarz, J.; Hecht, S.; Saalfrank, P. Quantum Chemical Investigation of Thermal Cis-to-Trans Isomerization of Azobenzene Derivatives: Substituent Effects, Solvent Effects, and Comparison to Experimental Data. *J. Phys. Chem. A* **2009**, *113* (24), 6763−6773.
(24) Garcia-Amoros, J.; Sanchez-Ferrer, A.; Massad, W. A.; Nonell, S.; Velasco, D. Kinetic Study of the Fast Thermal Cis-to-Trans Isomerisation of Para-, Ortho- and Polyhydroxyazobenzenes. *Phys. Chem. Chem. Phys.* **2010**, *12* (40), 13238−13242.
(25) Krylova, I. Painting by Electrodeposition on the Eve of the 21st Century. *Prog. Org. Coat.* **2001**, *42* (3−4), 119−131.
(26) Chappaz-Gillot, C.; Berson, S.; Salazar, R.; Lechêne, B.; Aldakov, D.; Delaye, V.; Guillerez, S.; Ivanova, V. Polymer Solar Cells with Electrodeposited CuSCN Nanowires as New Efficient Hole Transporting Layer. *Sol. Energy Mater. Sol. Cells, Part A* **2014**, *120*, 163−167.
(27) Musselman, K. P.; Wisnet, A.; Iza, D. C.; Hesse, H. C.; Scheu, C.; MacManus-Driscoll, J. L.; Schmidt-Mende, L. Strong Efficiency Improvements in Ultra-Low-Cost Inorganic Nanowire Solar Cells. *Adv. Mater.* **2010**, *22* (35), E254−E258.
(28) Park, C. W.; Kang, S.-K.; Hernandez, H. L.; Kaitz, J. A.; Wie, D. S.; Shin, J.; Lee, O. P.; Sottos, N. R.; Moore, J. S.; Rogers, J. A.; White, S. R. Thermally Triggered Degradation of Transient Electronic Devices. *Adv. Mater.* **2015**, *27* (25), 3783−3788.
(29) Dicheva, B. M.; ten Hagen, T. L. M.; Li, L.; Schipper, D.; Seynhaeve, A. L. B.; van Rhoon, G. C.; Eggermont, A. M. M.; Lindner, L. H.; Koning, G. A. Cationic Thermosensitive Liposomes: A Novel Dual Targeted Heat-Triggered Drug Delivery Approach for Endothelial and Tumor Cells. *Nano Lett.* **2013**, *13* (6), 2324−2331.
(30) Pakula, C.; Hanisch, C.; Zaporojtchenko, V.; Strunskus, T.; Bornholdt, C.; Zargarani, D.; Herges, R.; Faupel, F. Optical Switching Behavior of azobenzene/PMMA Blends with High Chromophore Concentration. *J. Mater. Sci.* **2011**, *46* (8), 2488−2494.
(31) Monguzzi, A.; Mauri, M.; Bianchi, A.; Dibbanti, M. K.; Simonutti, R.; Meinardi, F. Solid-State Sensitized Upconversion in Polyacrylate Elastomers. *J. Phys. Chem. C* **2016**, *120* (5), 2609−2614.
(32) Wu, M.; Congreve, D. N.; Wilson, M. W. B.; Jean, J.; Geva, N.; Welborn, M.; Van Voorhis, T.; Bulović, V.; Bawendi, M. G.; Baldo, M. A. Solid-State Infrared-to-Visible Upconversion Sensitized by Colloidal Nanocrystals. *Nat. Photonics* **2016**, *10* (1), 31−34.
(33) Lee, S. H.; Ayer, M. A.; Vadrucci, R.; Weder, C.; Simon, Y. C. Light Upconversion by Triplet-Triplet Annihilation in Diphenylanthracene-Based Copolymers. *Polym. Chem.* **2014**, *5* (24), 6898−6904.
(34) Kolpak, A. M.; Grossman, J. C. Hybrid Chromophore/template Nanostructures: A Customizable Platform Material for Solar Energy Storage and Conversion. *J. Chem. Phys.* **2013**, *138* (3), 034303.

DOI: 10.1021/acsami.6b08034
ACS Appl. Mater. Interfaces 2016, 8, 26319−26325